ITALIAN NATIONAL AGENCY FOR NEW TECHNOLOGIES, ENERGY AND SUSTAINABLE ECONOMIC DEVELOPMENT

TOR VERGATA
UNIVERSITÀ DEGLI STUDI DI ROMA
Department of Industrial Engineering

CVD Diamond Detectors for Fast VUV and SX-Ray Tomography

Proposal for the IO - ITPA Diagnostics TG

Cadarache 25-28 October 2021

F. Bombarda, M. Angelone, G. Apruzzese, G. Pucella, *ENEA-FSN* Frascati (RM), Italy

S. Cesaroni, M. Marinelli, E. Milani, S. Palomba, C. Verona, G. Verona-Rinati,
Dept. of Ind. Eng., U. of Rome "Tor Vergata," Rome, Italy

Frascati, 12/10/2021

CVD Diamonds for UV and SX photon detection

Developed and custom grown at “Tor Vergata” University in Rome

Chemical Vapour Deposition (CVD) single crystal diamonds exhibit excellent photon detection properties :

- Wide band gap (5.5.eV) → low leakage current and sensitivity to photon $\lambda < 225$ nm (visible blind)
- High carrier mobility → fast time response (< 1 ns)
- High thermal (tested up to 625 K) and mechanical resistance
- Good radiation hardness > Si photodiodes; measured at FNG up to 2×10^{14} (14 MeV n/cm^2) with no degradation
- High Vacuum compatible → No Be windows required

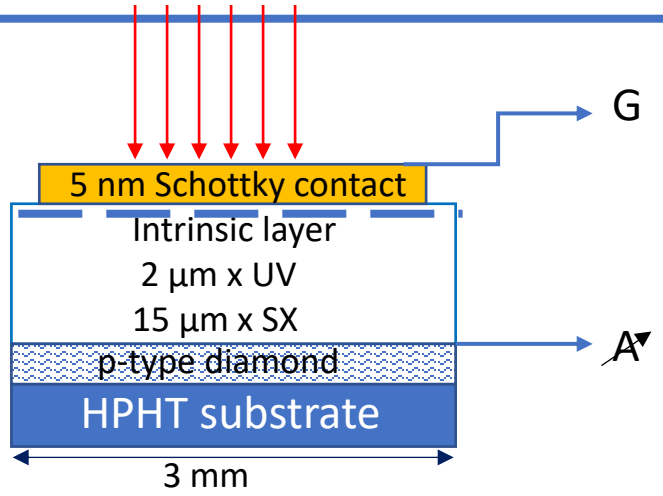

Multilayer planar configuration

p-type/intrinsic/Schottky metal contact configuration
Intrinsic layer thickness = 2 – 50 µm for super-high quality
B doping for p-type layer
Top metal contact : Pt, Cr, Al et al, variable thickness
Bias Voltage 0 – 10 V

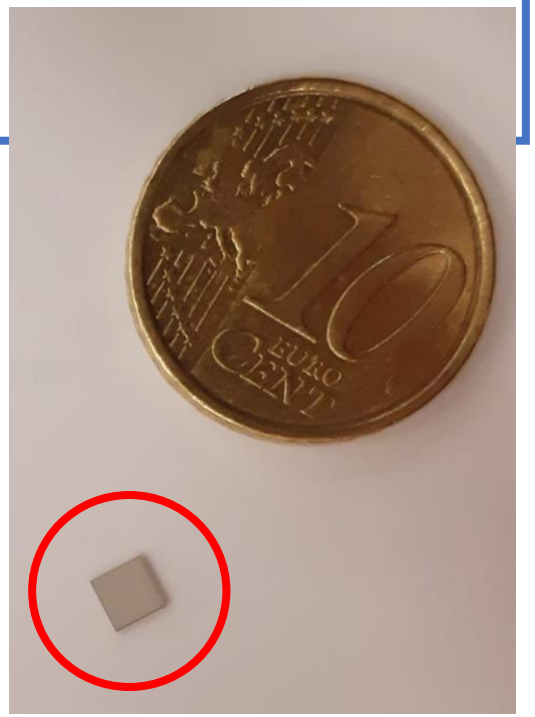

JET layout

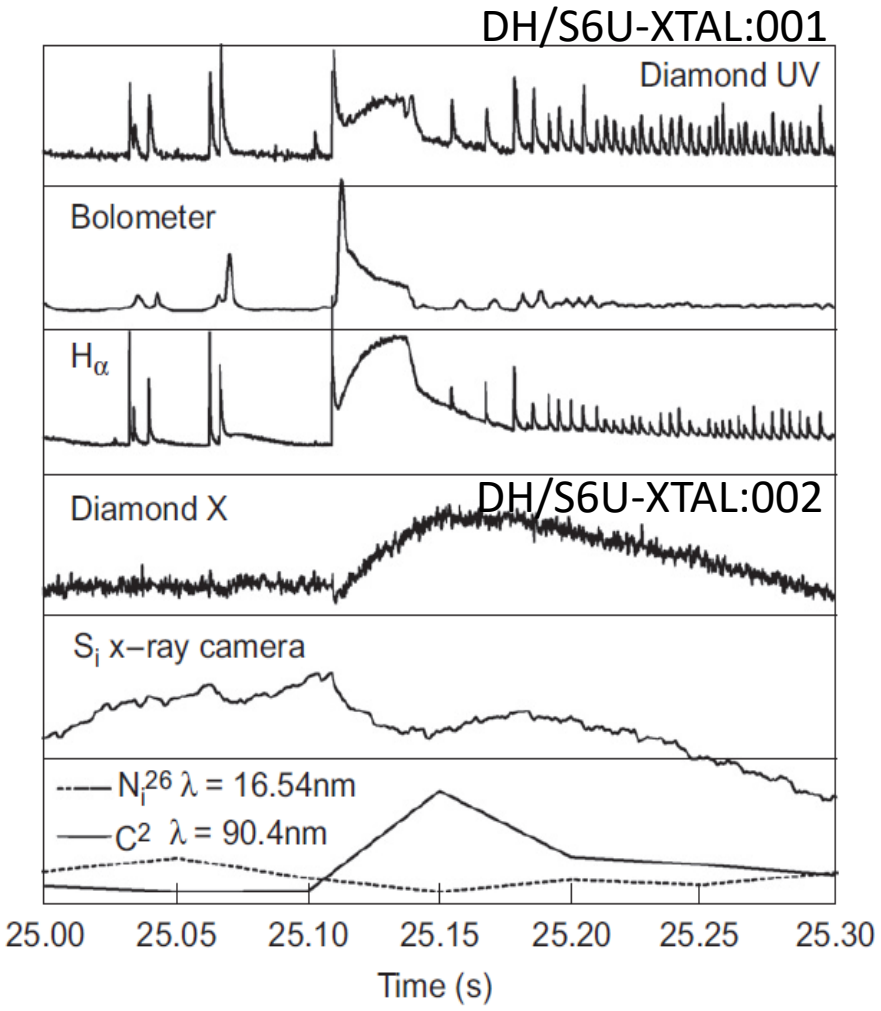

Fig. 5. Measurements during a carbon impurities influx.

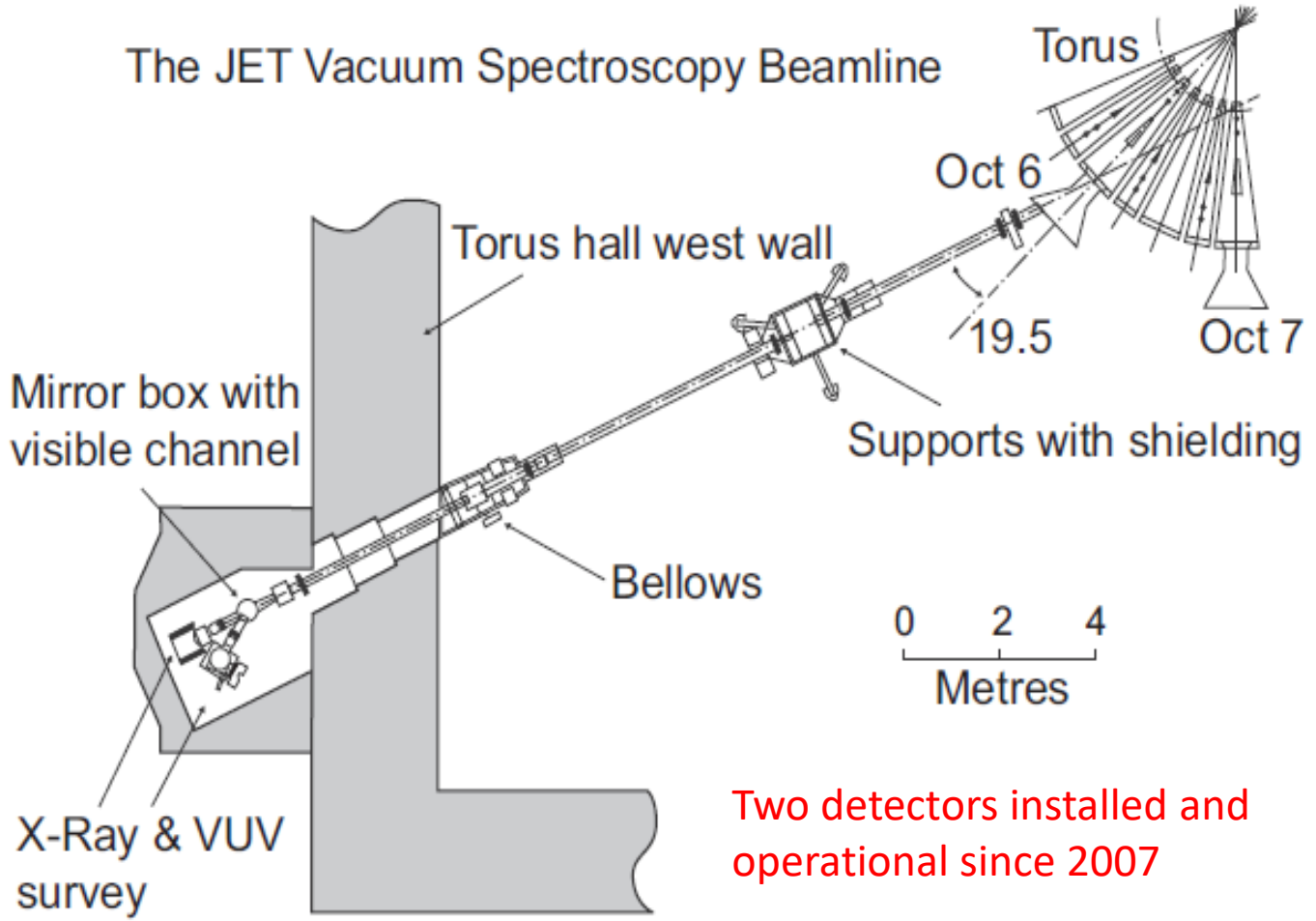

Two detectors installed and operational since 2007

Fig. 3. Location of JET VUV and softX survey spectrometer. The bunker is shared with a Bragg rotor X-ray spectrometer and a visible channel.

Nuclear Instruments and Methods in Physics Research A 623 (2010) 726–730

M. Angelone [a], M. Pillon [a,*], Marco Marinelli [b], E. Milani [b], G. Prestopino [b], C. Verona [b], G. Verona-Rinati [b], I. Coffey [c], A. Murari [d], N. Tartoni [e], JET-EFDA contributors [f,1]

CVD Diamond for UV and SX on FTU (2019)

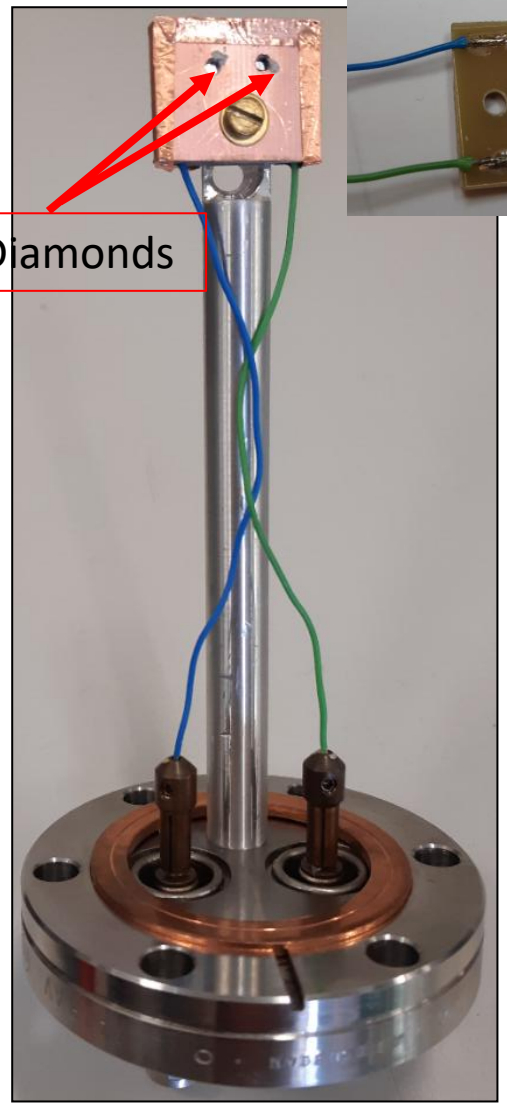

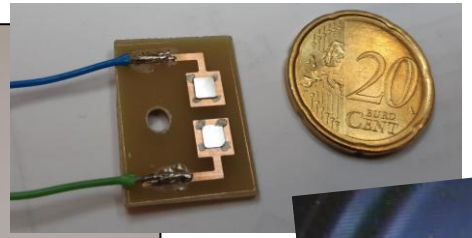

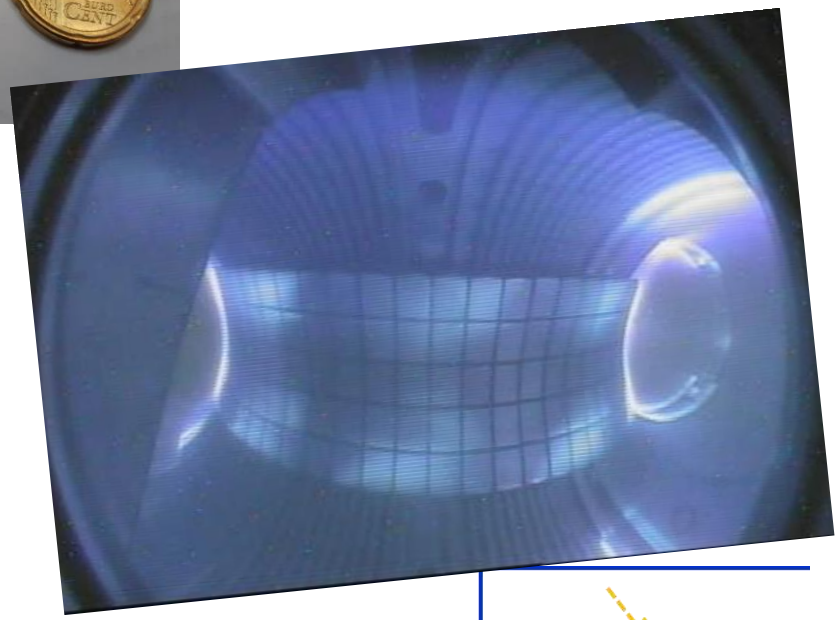

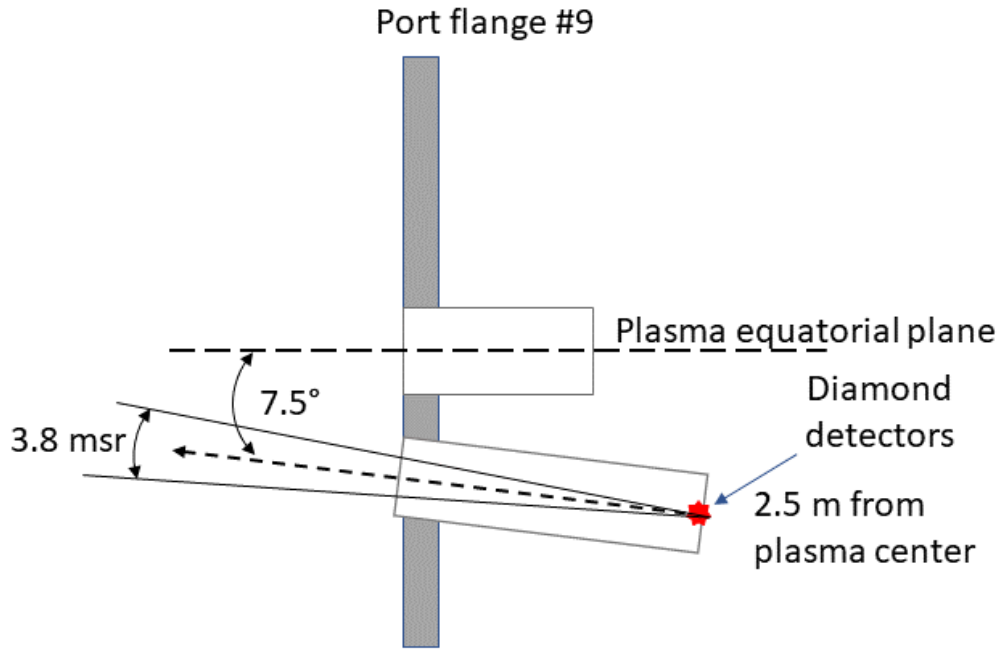

UV: 2µm, 5nm of Pt

SX: 15µm, 5nm of Cr + 6µm of Mylar filter

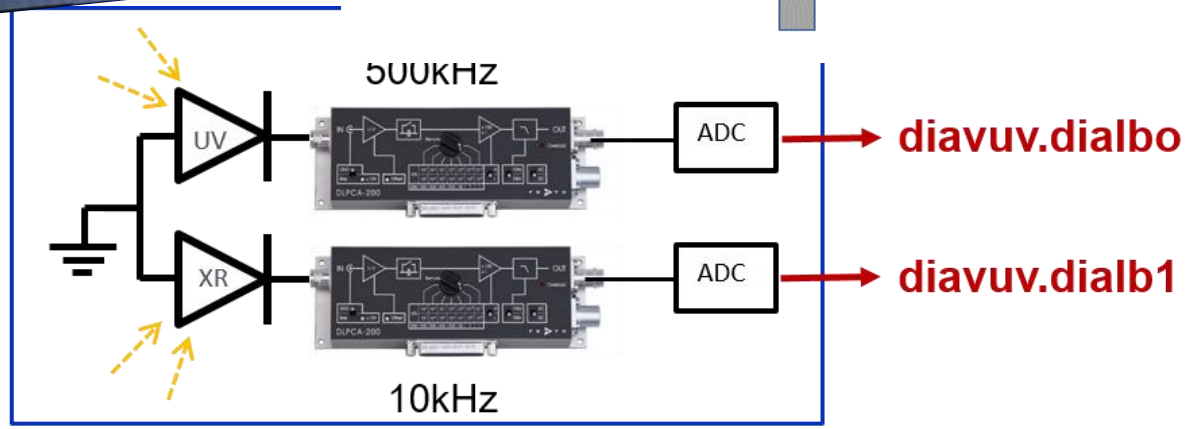

S. Cesaroni et al., *Fus. Eng. & Design* **166** 112323 (2021)

FAST PLASMA PHENOMENA: pellet ablation

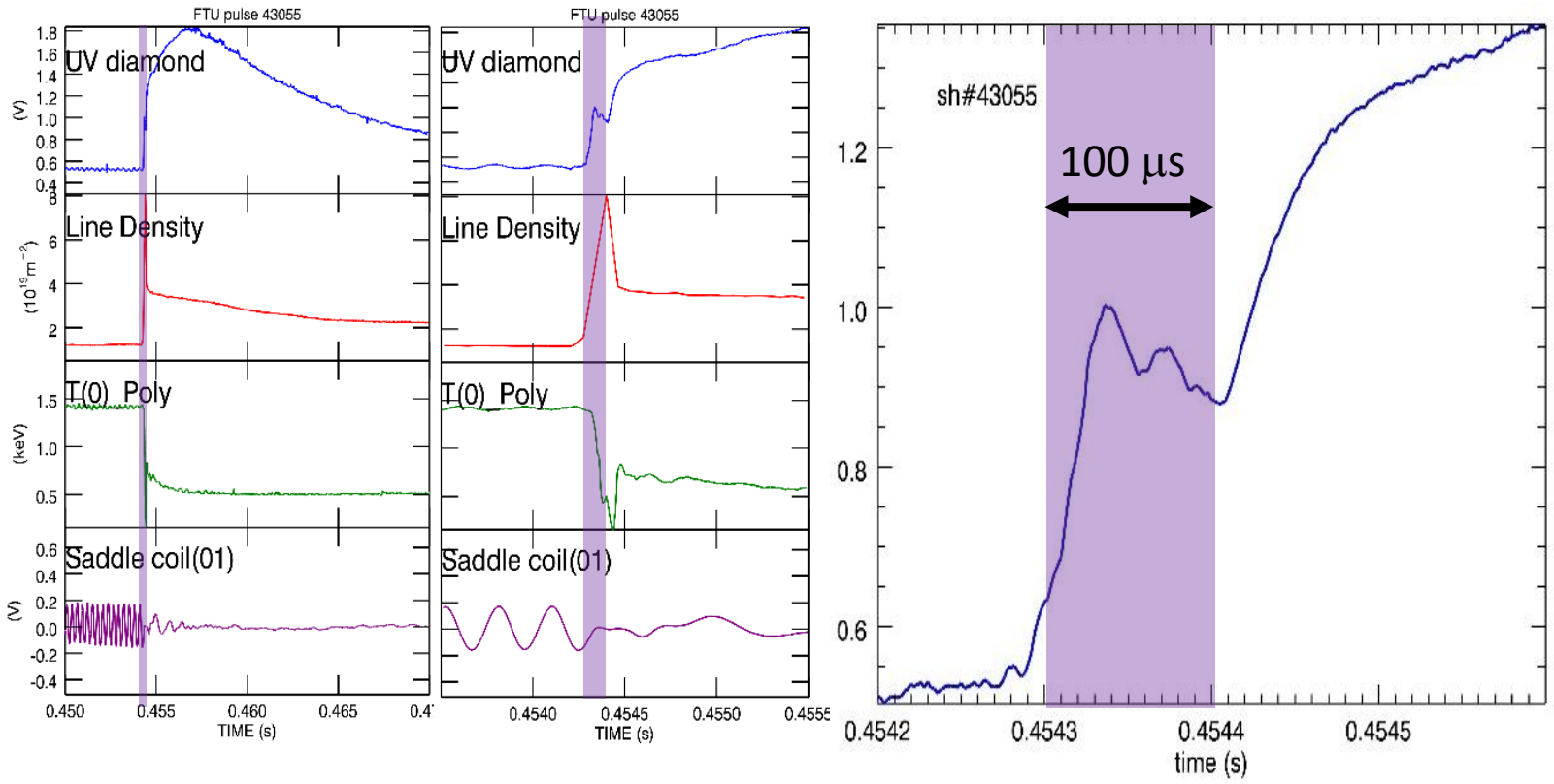

Figure 4 Ablation phase of a D pellet injected at about 1.2 km/s from the low field side midplane. The first column covers 20 ms from the injection trigger of the UV diamond signal, the line average density at R=1.1 m, the central channel of the ECE polychromator, and one of the saddle coils measuring the derivative of the radial magnetic field perturbations associated to MHD instabilities; the second column is an expanded view of the same signals; on the right 0.4 ms of the UV signal with the actual ablation phase occurring during the shaded area.

F. Bombarda et al., 2021 *Nucl. Fusion* **61** 116004 (2021)

≈ ELMs

-LoS NOT in direct view of pellet (unlike JET)

-Plasma radiation is a combination of:

A) Bremsstrahlung

B) Radiative recombination

C) Line radiation

$$\frac{dP}{dE_\nu} \propto n_e n_{Zi} f(T_e)$$

-Each phenomenon takes place on its own temporal and spatial scale

Mode locking and MARFEs

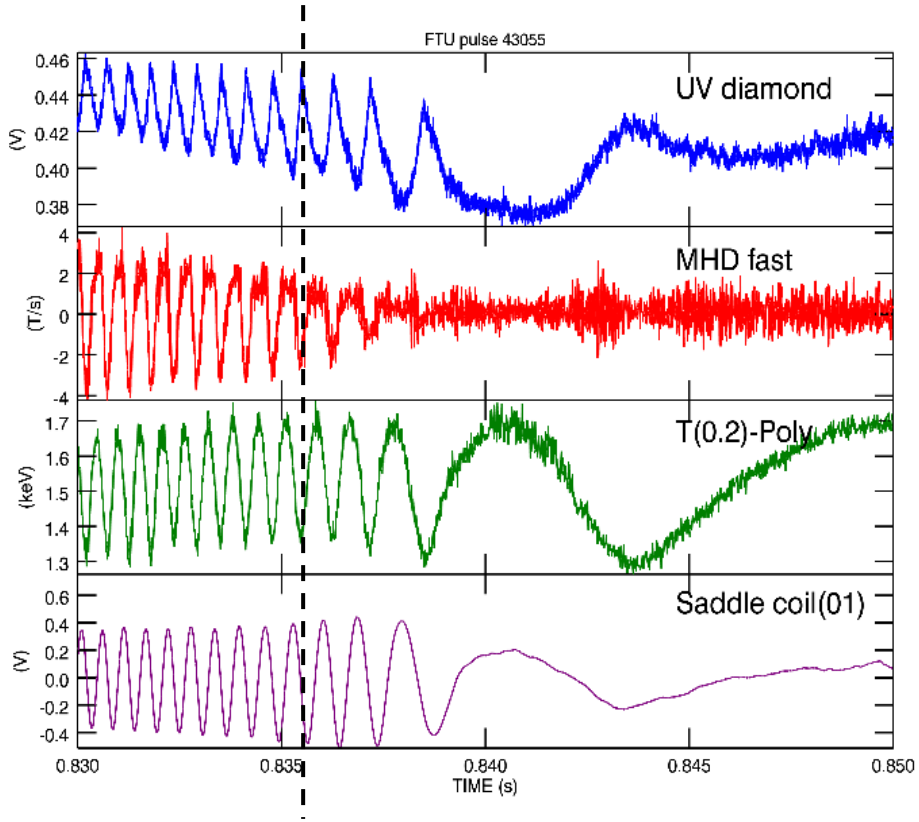

Example of rotating 2/1 tearing mode slowing down and locking as seen by different fast diagnostics. From the top: the UV diamond detector, a pick-up coil, the ECE polychromator temperature at r/a=0.2, and a saddle coil channel.

Poloidal (Mirnov) and radial (saddle) coils record the edge magnetic field perturbations induced by the tearing instability; ECE and UV signals are sensitive to local temperature profile perturbations associated to the island. For large islands caused the flattening of the parallel thermal conductivity is predominant over the perpendicular one.

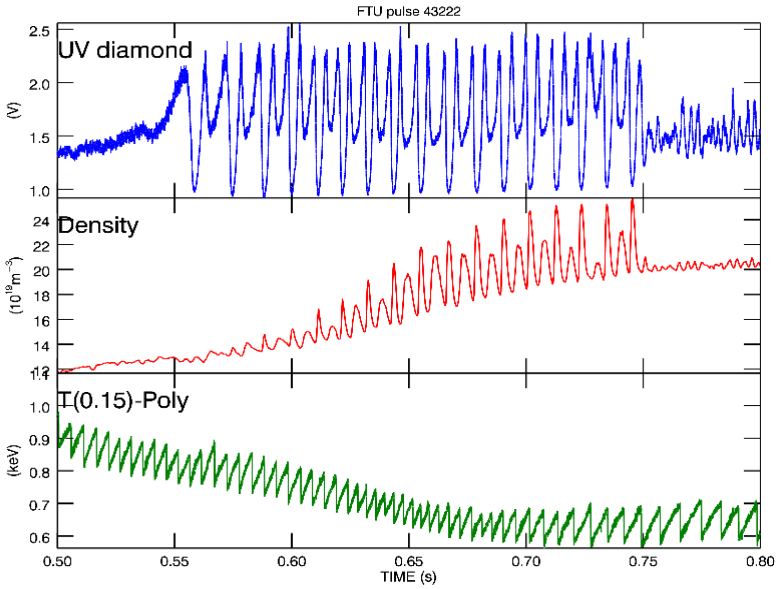

The UV diamond signal and the central line average density move in opposition, as expected; the core ECE polychromator channel continues sawtoothing at a frequency essentially double that of the MARFE.

MARFE oscillations as observed by the UV diamond, the line average density measured by the vertical central chord of the interferometer, and the ECE polychromator temperature at r/a=0.15.

CVD diamond-based bolometry

Thicker detectors can provide complementary information to conventional bolometers

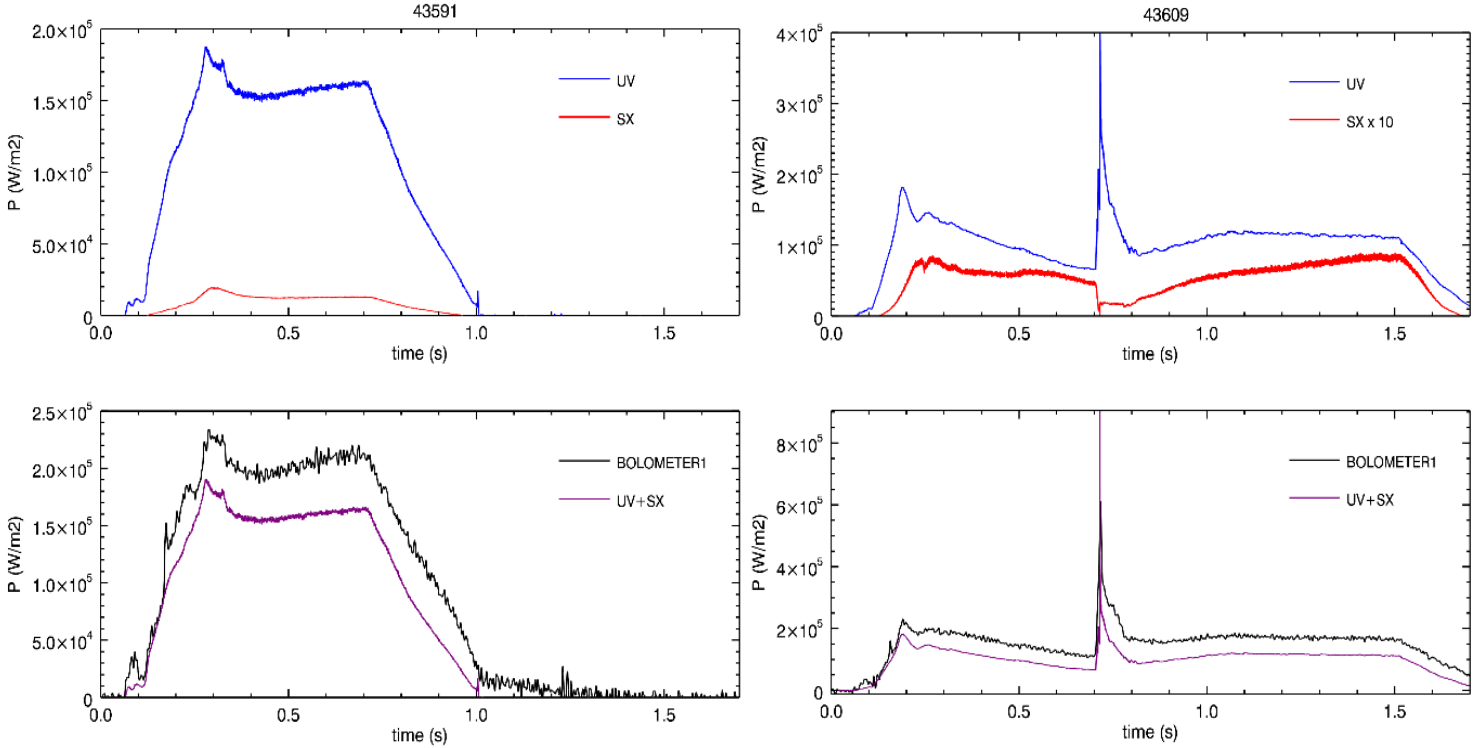

Comparison of radiated power densities from one of the calibrated bolometer channels and the combined signals from the UV and SX diamonds for two FTU discharges: a standard Ohmic discharge at 5 T, 550 kA, $n_e=5\times10^{19}m^{-3}$ (left), and one at 5 T, 360 kA, $n_e=1.3\times10^{19}m^{-3}$ with a single pellet injection (right). The top plots show the time traces of the two diamond detectors UV and SX, the bottom ones the comparison of their sum with the bolometer channel with a similar line-of-sight.

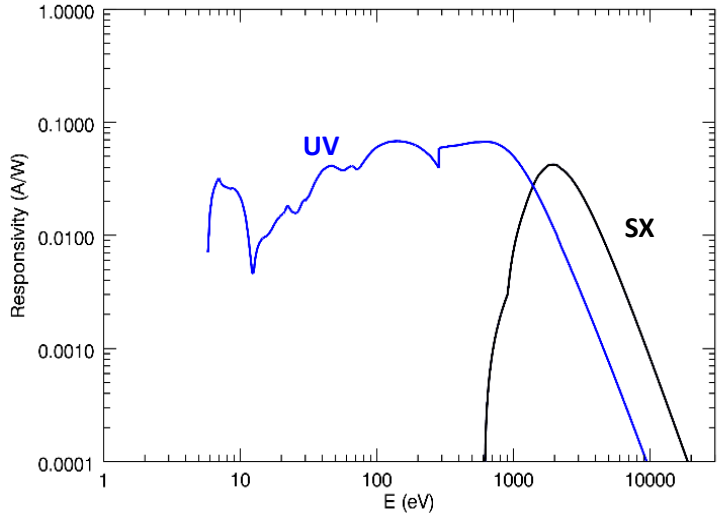

TOP: Calculated responsivity curves for the actual geometry of the detectors used on FTU; the calculation includes the Pt and Cr 5 nm contact layers, and the 6 mm Mylar filter for the SX detector.

BOTTOM: Calculated responsivity for thicknesses up to 9 mm

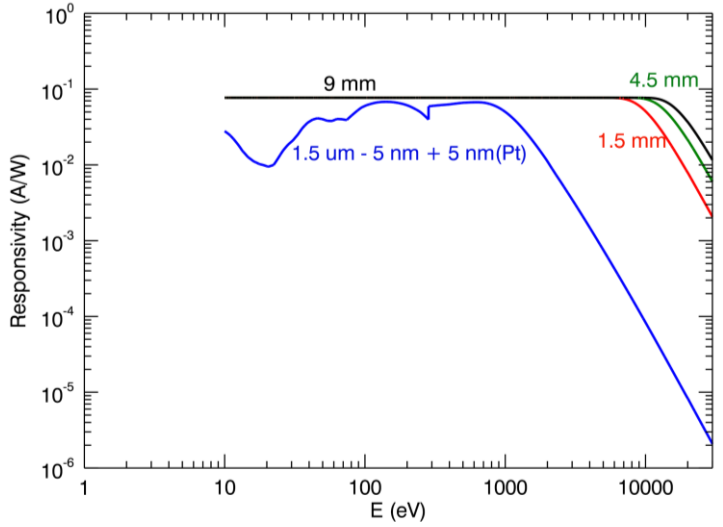

iDTT Tentative layout for diamond SX Tomography

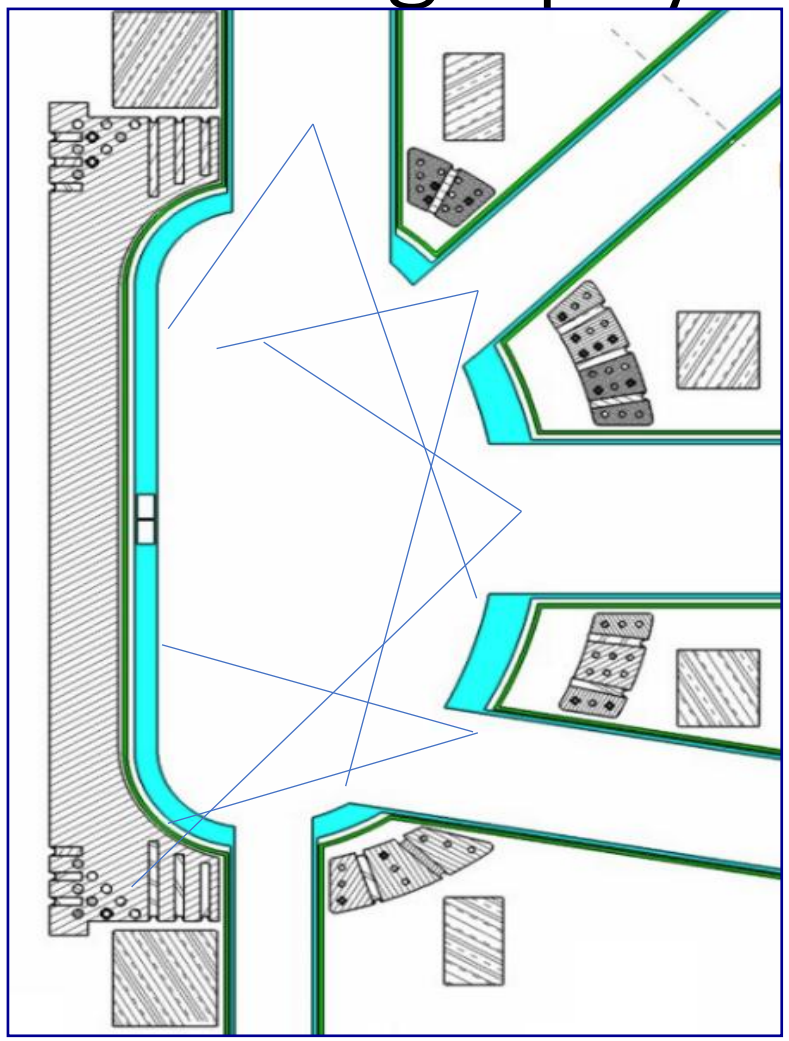

Thanks to the relatively low cost and extremely reduced dimensions large arrays can be envisaged for positioning close to the plasma, even in the presence of high neutron fluxes.

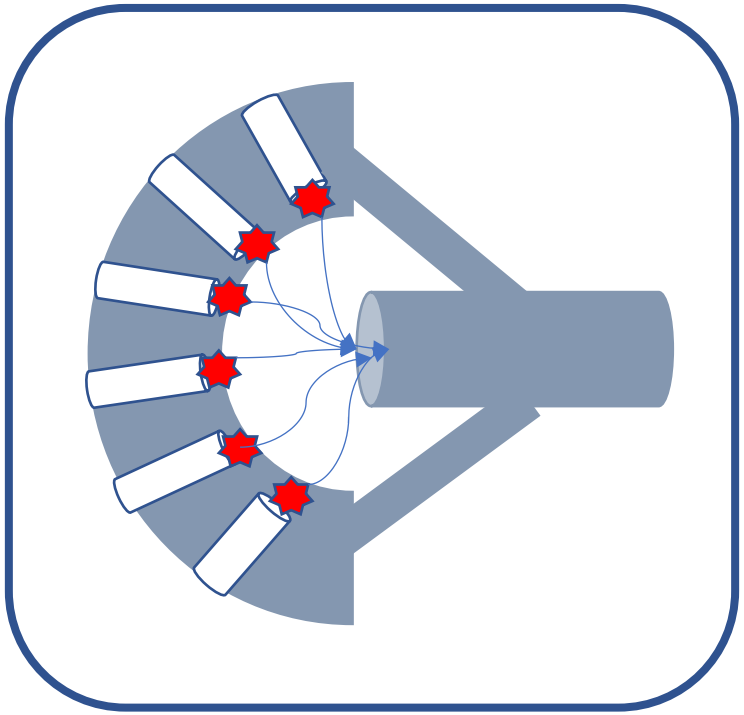

Appropriate detectors geometries will provide selective monitoring of edge/core features with poloidal/toroidal coverage

F. Bombarda

CVD diamonds for UV-SX tomography/bolometry in ITER

ITER diagnostic systems

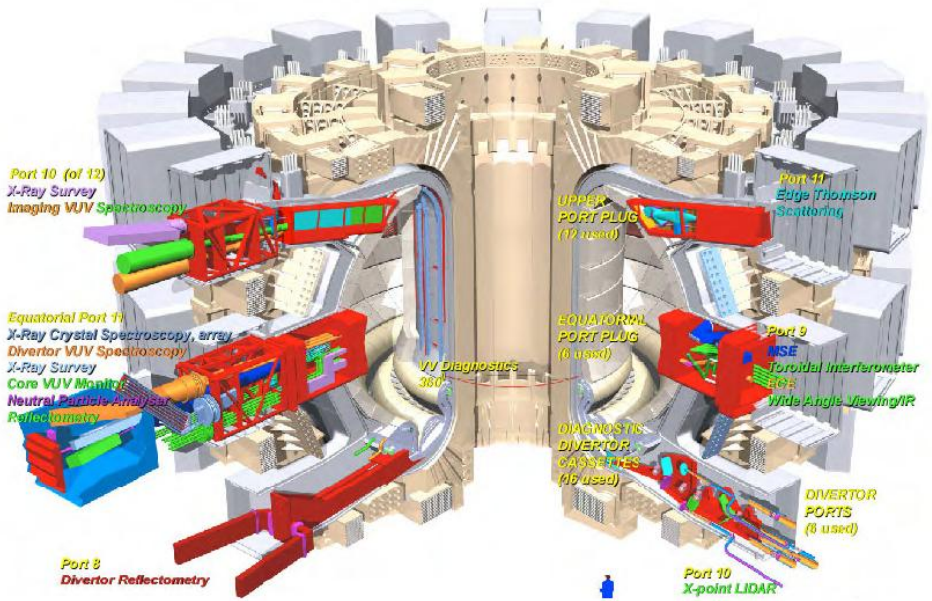

The ITER environment (2): radiation loads

Radiation loads (values corresponding to a fusion power of 700 MW):

- neutrons and gammas
- particles escaping plasma
- plasma radiation (synchrotron, bremsstrahlung, line radiation): x-rays–microwaves ; mainly VUV

Location	Typ. diagnostic components	Neutrons n/m²s		Dose rate Gy/s	Fluence (>0.1 MeV) n/m²	Particle flux atoms/m²s	Plasma radiation (peak) kW/m²
		>0.1 MeV	14 MeV				
First wall		3×10^{18}	8×10^{17}	2×10^{3}	3×10^{25}	$\sim5\times10^{19}$	500
Near blanket gap (on vacuum vessel)	magnetic coils, bolometers, retroreflectors	0.2×10^{16} – 1×10^{17}	0.8×10^{16} – 4×10^{16}	20 – 100	$0.2 – 2\times10^{24}$	$\sim10^{18}$	10
Vacuum vessel (behind blanket)	magnetic loops	2×10^{16}	3×10^{14}	≤ 20	2×10^{23}	~ 0	~ 0
Diagnostic block	First mirrors	1×10^{16}	9×10^{15}	20	1×10^{23}	$\sim10^{17}$	~ 1.5
Labyrinth	Second mirrors, windows	2×10^{13}	3×10^{13}	10^{-2}	2×10^{20}	~ 0	~ 0
Vacuum vessel (inboard TFC side)	magnetic loops	1×10^{14}	1×10^{12}	~ 0	$\sim10^{21}$	~ 0	~ 0
Divertor cassette	First mirrors	1×10^{18}	3×10^{17}	1×10^{-3}	$\sim10^{25}$	$10^{17} – 10^{19}$	1 – 100
Divertor port	Second mirrors	$10^{13} – 10^{15}$	$10^{12} – 10^{14}$	10^{-2} – 1	$10^{19} – 10^{21}$		

1Gy (Gray) = 1J of ionising radiation/kg

From: ITER DIAGNOSTICS/ Doctoral course on Plasma Diagnostics 2009/ H. Weisen, CRPP-EPFL

Bolometry

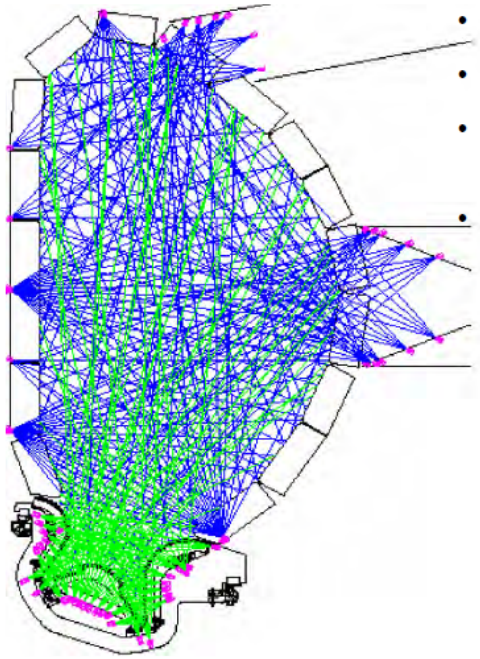

- Total radiated power measurement, tomography
- No lack of ambition here!
- Traditional type with Au as in TCV, AUG not radiation hard (Au→Hg!)
- Alternative with Pt on ceramic substrate ok at 0.01dpa

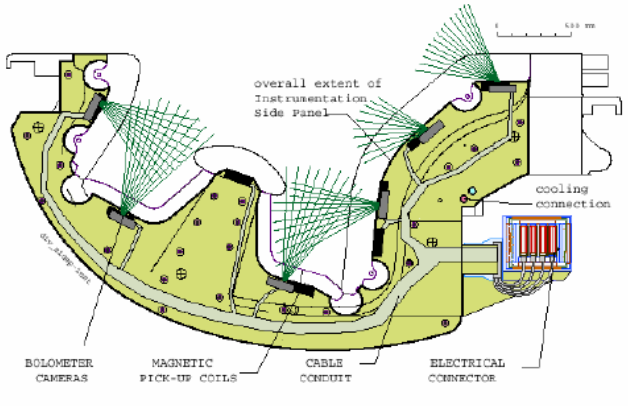

From: ITER DIAGNOSTICS/ Doctoral course on Plasma Diagnostics 2009/ H. Weisen, CRPP-EPFL

SUMMARY

- CVD single crystal diamonds are highly suitable for VUV and SX-ray in-vessel diagnostics of fusion plasmas in a variety of applications
- Radiation and temperature hardness, small size, and high-vacuum compatibility of diamonds can be exploited for core and divertor tomography/bolometry over a wide energy range (5.5 eV – 30 keV)
- Their fast response (in the ns range) can be applied for monitoring fast plasma events, such as ELMs, MHD instabilities, pellet ablation…
- The high-quality CVD diamond detectors developed and grown at “Tor Vergata” University in Rome have long been in use at JET and were more recently tested on FTU. Their deployment on DTT is under design
- Their application on ITER to complement/improve planned systems can be proposed.